



CrossMark  
 click for updates

Cite this: *RSC Adv.*, 2015, 5, 13068

# Comparative evaluation of the blends of gas-to-liquid (GTL) fuels and biodiesels with diesel at high idling conditions: an in-depth analysis on engine performance and environment pollutants

S. Hossain,\* H. H. Masjuki,\* M. Varman, M. A. Kalam and S. M. Ashrafur Rahman

This study focuses on the physicochemical fuel characteristics and engine performance-emission features of three prospective alternative transportation fuels: Alexandrian laurel biodiesel (ALBD), jatropha biodiesel (JBD) and GTL fuel at high idling conditions. The blends of GTL fuel (G10, G20), JBD (J10, J20) and ALBD (AL10, AL20) with diesel had been investigated in a multi-cylinder diesel engine at different load-speed conditions. Analysis of the fuel properties showed a linear variation of the major fuel properties with an increase of alternative fuel quantity in the blends. Engine performance test results revealed an average decrease of brake specific fuel consumption (BSFC) (ca. 8.65–12.26%) and brake specific energy consumption (BSEC) (ca. 8.27–11.51%), but a higher brake thermal efficiency (BTE) (ca. 8.56–12.58%) by GTL blends, whereas, the biodiesel blends showed higher BSFC (ca. 5.01–12.18%) and BSEC (ca. 3.41–9.67%) and lower BTE (ca. 3.68–9.93%), respectively, than those of diesel. Referring to the emission analysis, the results revealed that GTL blends showed a slight reduction in NO<sub>x</sub> (ca. 3.89–6.85%), but a significant reduction in CO (ca. 48.25–51.38%), HC (ca. 44.81–51.43%) and smoke (ca. 15.21–18.78%), respectively, when compared to diesel. The biodiesel blends demonstrated reduced CO (on average ca. 29.12–33.71%), HC (ca. 29.67–35.46%) and smoke (ca. 2.49–6.87%), but increased NO<sub>x</sub> (on average ca. 2.83–9.81%), respectively, than those of diesel.

Received 12th December 2014  
 Accepted 9th January 2015

DOI: 10.1039/c4ra16239k

[www.rsc.org/advances](http://www.rsc.org/advances)

## 1. Introduction

### 1.1. Background

Worldwide petroleum upheaval and environmental distress have heightened the urge for research and development of alternative fuels in the transportation sector. Biodiesel and gas-to-liquid (GTL) fuel can be considered as prospective future transportation fuels. Biodiesel is defined as the mono-alkyl esters of fatty acids, which can be extracted from vegetable oils, animal fats and alcohol. It has special features such as being renewable, biodegradable and free from toxicity; contains a higher cetane number (CN) and flash point, has inherent lubricity and demonstrates more diminution in emissions, when compared with fossil diesel.<sup>1,2</sup> *Jatropha curcas* and Alexandrian laurel can be regarded as potential feedstock for biodiesel production because of their non-edible origin, higher oil yield than other non-edible feedstocks and the compliance of the biodiesel yield from its crude oil with the US ASTM D6751 and European Union EN 14214 biodiesel standards.<sup>3,4</sup> GTL fuel can be synthesized in a number of ways, such as, the methane

reforming process, Fischer–Tropsch (FT) synthesis, and hydrocracking processes.<sup>5,6</sup> The FT synthesis converts a mixture of carbon monoxide and hydrogen into various liquid hydrocarbons, by using suitable catalysts.<sup>7</sup> GTL fuel possesses higher CN, virtually no sulfur and negligible amounts of aromatics<sup>8–10</sup> and also demonstrates significantly lower emission than diesel and biodiesel.<sup>11–13</sup> Thus, it can be regarded as a clean alternative fuel that can yield low exhaust emissions, without any major engine modifications and significant loss in efficiency. Previous studies regarding the engine performance-emission tests of alternative fuels like biodiesel, GTL and their blends with diesel, were only confined to some common test conditions, such as, full load or medium load and variation of engine speeds. Most of the studies<sup>14–19</sup> showed that biodiesel blends with diesel showed decreasing power, CO, HC and smoke emissions, whereas an increase was observed in fuel consumption and NO<sub>x</sub> emissions. The research<sup>8–10,20</sup> in GTL–diesel blends reported that blending GTL fuel with diesel can certainly improve the fuel properties of the blends, which lead towards better engine performance and exhaust emission than diesel.

The effect of idling conditions on alternative fuels at major engine performance-emission parameters should also be considered as a significant research scope, which has not yet

Centre for Energy Sciences, Department of Mechanical Engineering, Faculty of Engineering, University of Malaya, 50603 Kuala Lumpur, Malaysia. E-mail: s.hossainme@gmail.com; masjuki@um.edu.my; Fax: +603 79675317

been investigated thoroughly. Idling refers to the incessant operation of the primary propulsion engine of any automobile during its stationary position. Generally, automotive engines switch to idling modes in traffic ambiances, particularly at traffic signals and intermittent driving during traffic jam in urban areas. However, the duration of engine idling in these conditions is short compared to the idling state of heavy-duty diesel engines whilst parked during journey intervals on highways with running engines to utilize the air conditioning. Idling results in emission of harmful environmental pollutants and also a significant increase in fuel consumption. A number of studies<sup>21–24</sup> on the idling effects on diesel fuel have been reported in the last decades. As the blends of alternative fuel and diesel are being considered as prospective transportation fuels, a comparative analysis of these blends will be of great significance to study their performances at high idling conditions. When the engine is operated at low load-low rated speed conditions, it is regarded as high idling condition.<sup>25</sup> At these conditions, the engine cannot attain the required operating temperature, which leads to incomplete combustion. Thus, higher fuel consumption, associated with an increase in exhaust emissions have been observed in idling conditions. Regarding the high idling test conditions, only three studies<sup>26–28</sup> have been reported using diesel–biodiesel blends, but no study with GTL–diesel blends have been performed till now. The previous studies had some limitations. The comparative analysis of multiple alternative fuel blends were not illustrated. Besides, those studies did not include smoke emissions at high idling conditions.

### 1.2. Objective

The objective of this study is to investigate the idling effects of the six blends of JBD, ALBD and GTL fuel with diesel in the context of different engine performance-emission parameters at four different engine test conditions. This study of the idling effects on alternative fuel blends will provide a justification in commercial application of these fuels.

## 2. Experimental set up and procedures

### 2.1. Biodiesel production

The production process of biodiesel from crude oil depends on the free fatty acid (FFA) content of the crude oil. High FFA content leads to the occurrence of soap formation, which not only constrains the isolation process of the ester from glycerin, but also decreases the transformation rate of ester. According to Canakci and Van Garpen,<sup>29</sup> oils with FFA higher than 1%, which illustrates the acid value of 2 mg KOH per g is not susceptible to the alkaline-catalyzed trans-esterification process. *Jatropha curcas* and Alexandrian laurel crude oil have an FFA content of 8% (acid value 16 mg KOH per g) and 20% (acid value 40 mg KOH per g), respectively. So, acid-catalyzed esterification should be applied at first for both of these crude oils to reduce the FFA level.<sup>30</sup> After that the alkali-catalyzed trans-esterification process can be applied. At first, crude oil was placed in a jacket reactor

of 1 liter capacity, equipped with an IKA Eurostar digital model stirrer and Wiscircu water bath arrangement. Next, methanol (in 12 : 1 molar ratio) and H<sub>2</sub>SO<sub>4</sub> (1% v/v) were added. The system was kept at a temperature of 50–60 °C for 3 hours by circulation of hot water through the jacket, while stirring at a constant speed of 1100 rpm. To check the change in FFA level, a 5 mL sample was collected at regular 10 minute intervals and the process was continued until the FFA level had decreased by 1–2%. After the completion of acid esterification, the mixture was poured into a separation funnel to isolate the esterified product and catalyst layer. The catalyst layer contained excess H<sub>2</sub>SO<sub>4</sub> and alcohol, and was found to be the upper layer. After isolation, the lower layer was extracted and placed into a rotary evaporator to eliminate excess methanol and water. The yield from this process is approximately 98%.<sup>31</sup> After the completion of acid esterification, the product was subjected to alkali-catalyzed trans-esterification.

In the alkali-catalyzed trans-esterification process, methanol (25% v/v oil) and potassium hydroxide 1% (w/w oil) were added, with the esterified oil, to the biodiesel reactor. This mixture was stirred at 60 °C for 3 hours, maintaining a speed of 1000 rpm. After that the mixture was transferred to a separation funnel, where it appeared as two layers of glycerol impurities (lower layer) and methyl esters (upper layer). Eventually, the lower layer was isolated and the upper layer was cleansed thoroughly by spraying 50% (v/v) hot (50 °C) distilled water over the methyl esters while shaking gently to ensure proper washing. The cleansing process was repeated until the methyl ester achieved a pH value of 7. Excess water and methanol content were removed from the methyl ester by using an IKA RV10 rotary evaporator. For moisture removal from the methyl ester, anhydrous sodium sulfate was used. Finally, the methyl ester was obtained by filtration using high quality filter papers.

### 2.2. GTL production process

GTL production stages can be sub-categorized as formation of synthesis gas (syngas), catalytic synthesis (conversion of syngas) and the post processing (cracking). Syngas can be formed from any carbonaceous elements such as: natural gas, petroleum coke coal or biomass. At first, carbon and hydrogen are differentiated from methane. After that, they are transformed in several processes available for syngas production depending on the feed stock, such as partial oxidation, steam reforming, auto thermal reforming (ATR), gasification and a combination of those, which result in different ratios of hydrocarbon–carbon monoxide. In a catalytic synthesis process, the gaseous mixture of CO and H<sub>2</sub> (syngas) is processed in various Fischer–Tropsch reactors and yields long-chain, waxy hydrocarbons and a considerable quantity of water as by-product. The reactors used in catalytic synthesis are specified by different designs targeting the technology to produce a wide ranges of paraffinic long-chain hydrocarbons (synthetic crude). Finally, this synthetic crude is processed through traditional refinery cracking operations in the presence of zeolite catalysts and hydrogen to yield catalytically cracked shorter hydrocarbons. These shorter hydrocarbons undergo distillation to produce GTL fuels.<sup>32</sup>

### 2.3. GC analysis and fatty acid composition of fuels

Gas chromatographic (GC) analysis was performed to investigate the fatty acid composition of the produced biodiesel. A sample of 1  $\mu\text{L}$  was injected into a Shimadzu GC-2010A series chromatography panel. The specifications of the instrument and operation conditions are presented in Table 1. The fatty acid composition of the produced biodiesel fuels is presented in Table 2. The test results showed that JBD contains saturated methyl esters (*ca.* 24.3%), mono-saturated methyl esters (*ca.* 42.6%), and poly-unsaturated methyl esters (*ca.* 33.1%).

### 2.4. Fuel blend preparation and properties analysis

In this study, six blends were prepared as sample fuels. JBD, ALBD and GTL fuels were mixed with diesel in two ratios, 1 : 9 and 1 : 4. The sample blend with 10% (by vol) of JBD, ALBD or GTL fuel with 90% diesel were named J10, AL10 and G10, respectively. Similarly, the blends containing 20% biodiesel or GTL fuel and 80% diesel were named J20, AL20 and G20, respectively. While preparing the blend, the calculated volumes of diesel and other test fuel were first taken into a sealed magnetic stirrer and next in a shaker. Each of the test sample

fuel blends was stirred at 4000 rpm for 30 minutes. Then the stirred blend was placed in the digital shaker for additional 30 minutes at 400 rpm. Finally, the blend sample was removed from the shaker and observed for 12 h to ensure that no phase separation was occurring. The apparatus for fuel property analysis are shown in Table 3. The fuel properties of the produced biodiesel are listed in Table 4. In this table, saponification number (SN), iodine value (IV) and cetane number (CN) were calculated by using the fatty acid composition results and the following empirical eqn (1)–(3),<sup>33</sup> respectively.

$$\text{SN} = \sum \frac{(560 \times A_i)}{\text{MW}_i} \quad (1)$$

$$\text{IV} = \sum \frac{(254 \times D \times A_i)}{\text{MW}_i} \quad (2)$$

$$\text{CN} = 46.3 + \frac{5458}{\text{SN}} - \frac{0.225}{\text{IV}} \quad (3)$$

where,  $A_i$  is the weight percentage of each fatty acid component,  $D$  is the number of double bonds present in each fatty acid and  $\text{MW}_i$  is the molecular weight of each fatty acid component.

Table 1 GC panel and operating conditions

Property	Specifications
Carrier gas	Helium, 83 kpa (split ratio 50 : 1)
GC column	BPX70, capillary type (30.0 m $\times$ 0.25 $\mu\text{m}$ $\times$ 0.32 mm, inner diameter)
GC column flow rate	1.10 mL min <sup>-1</sup>
Injector	Split/split less (type 1177) with EFC control
Injection volume	1 $\mu\text{L}$
Detector type	Flame ionization detector (FID), 250.0 $^\circ\text{C}$
<b>Operating temperatures</b>	
Oven	140.0 $^\circ\text{C}$
Injector	240.0 $^\circ\text{C}$
Detector ports	260.0 $^\circ\text{C}$
Initial hold	140.0 $^\circ\text{C}$ (hold for 2 minutes)
Temperature ramp (after initial hold)	8 $^\circ\text{C min}^{-1}$ to 165.0 $^\circ\text{C}$ 3 $^\circ\text{C min}^{-1}$ to 192.0 $^\circ\text{C}$ 8 $^\circ\text{C min}^{-1}$ to 220.0 $^\circ\text{C}$

Table 2 Fatty acid composition of biodiesel

Fatty acid ester	Structure	Molecular mass	Formula	ALBD	JBD
Methyl myristate	14:00	242.40	$\text{CH}_3(\text{CH}_2)_{12}\text{COOCH}_3$	0	0.1
Methyl laureate	12:00	214.34	$\text{CH}_3(\text{CH}_2)_{10}\text{COOCH}_3$	0	0.1
Methyl palmitate	16:00	270.45	$\text{CH}_3(\text{CH}_2)_{14}\text{COOCH}_3$	14.8	17.7
Methyl palmitoleate	16:01	268.43	$\text{CH}_3(\text{CH}_2)_5\text{CH}=\text{CH}(\text{CH}_2)_7\text{COOCH}_3$	0.3	0.8
Methyl stearate	18:00	298.50	$\text{CH}_3(\text{CH}_2)_{16}\text{COOCH}_3$	16	6.4
Methyl oleate	18:01	296.49	$\text{CH}_3(\text{CH}_2)_7\text{CH}=\text{CH}(\text{CH}_2)_7\text{COOCH}_3$	41.3	41.8
Methyl linoleate	18:02	294.47	$\text{CH}_3(\text{CH}_2)_3(\text{CH}_2\text{CH}=\text{CH})_2(\text{CH}_2)_7\text{COOCH}_3$	26.6	32.9
Methyl linolenate	18:03	292.46	$\text{CH}_3(\text{CH}_2\text{CH}=\text{CH})_3(\text{CH}_2)_7\text{COOCH}_3$	0.2	0.2
Methyl arachidate	20:0	326.56	$\text{CH}_3(\text{CH}_2)_{18}\text{COOCH}_3$	0.8	0.1
Methyl erucate	22:1	338	$\text{CH}_3(\text{CH}_2)_7\text{CH}=\text{CH}(\text{CH}_2)_{11}\text{COOH}$	0.5	0
Methyl eicosenoate	20:01	324.54	$\text{CH}_3(\text{CH}_2)_{16}\text{CH}=\text{CHCOOCH}_3$	0.2	0
Methyl behenate	22:00	354.62	$\text{CH}_3(\text{CH}_2)_{20}\text{COOCH}_3$	0	0
Methyl lignocerate	24:00	382.66	$\text{CH}_3(\text{CH}_2)_{22}\text{COOCH}_3$	0	0

Table 3 Equipment for fuel property testing

Properties	Equipment	Manufacturer	Standard method	ASTM D6751 limit	Accuracy
Kinematic viscosity	SVM 3000-automatic	Anton Paar, UK	D445	1.9–6.0	±0.35%
Density	SVM 3000-automatic	Anton Paar, UK		Not specified	±0.1 kg m <sup>-3</sup>
Flash point	Pensky-Martens flash point-automatic NPM 440	Normalab, France	D93	130 min	±0.1 °C
Calorific value	C2000 basic calorimeter-automatic	IKA, UK	D240	D6371	±0.1% of reading
Oxidation stability	873 Rancimat—automatic	Metrohm, Switzerland	D675	3 hour	±0.01 hour
Cloud point	Cloud and pour point tester—automatic NTE 450	Normalab, France	D2500	Report	±0.1 °C
Pour point	Cloud and pour point tester—automatic NTE 450	Normalab, France	D2500	Not specified	±0.1 °C
CFPP	Cold filter plugging point—automatic NTL 450	Normalab, France	D6371	Not specified	±0.1 °C
Acid value	G-20 Rondolino automated titration system	Mettler Toledo, Switzerland	D664	0.5 max	±0.001 mg KOH per g

Table 4 Physicochemical characteristics of crude oil and produced biodiesel

Properties	ASTM D6751	EN 14214	Crude jatropha oil	JBD	Crude AL oil	ALBD
Density@40 °C (g cm <sup>-3</sup> )	Not specified	860–900	918.9	878.8	921.6	877.0
Kinematic viscosity@40 °C (mm <sup>2</sup> s <sup>-1</sup> )	1.9–6.0	3.5–5.0	34.072	4.2684	53.136	5.6872
Flash point (°C)	>130	>120	210.5	176.5	218.5	141.5
Calorific value (MJ kg <sup>-1</sup> )	Not specified	Not specified	39.420	40.899	38.51	39.39
Cetane no.	≥47	>51	—	53.5	—	56.3
CP, (°C)	Report	Not specified	12	3	8	7
PP, (°C)	Not specified	Not specified	1	2	8	7
CFPP, (°C)	Not specified	Not specified	22	1	27	8
Acid value (mg KOH per g)	<0.50	<0.50	16	0.18	40	0.34
Saponification number	Not specified	Not specified	—	192.6	—	191.6
Iodine value	Not specified	Not specified	—	93.8	—	82.1
Oxidation stability at 110 °C, (h)	>3	>6	1.2	8.41	2.43	3.58

## 2.5. Engine test rig

A four-cylinder, four-stroke, water-cooled diesel engine was used for experimental investigation. The test engine was directly coupled to a Froude-Hoffman AG250 eddy current

dynamometer. The test rig schematic is shown in Fig. 1. The specifications of the test engine and experimental conditions are shown in Table 5. The initial engine run was performed with diesel before starting the tests with all sample fuels. Before starting the test with sample test fuels, the engine was run for ten minutes to ensure removal of any residual diesel. After the test of each sample fuel, the fuel line was purged with diesel to remove that sample and to make it ready for the next sample. This procedure had been maintained for testing in all test conditions. The operations were performed at the same injection timing for all tested fuels.

In this study, four sets of test conditions were selected. At first, the engine test was performed at 10% load at 1000 rpm and 1500 rpm speed. Then at 15% load at 1000 rpm and 1500 rpm speed. To maintain accuracy, each test point was repeated thrice and the mean value was obtained to plot graphs. Each set of test conditions was given a name for convenience and these are shown in Table 5. In addition, each and every test data series (*i.e.* test point with the same fuel type and at various engine conditions) was recorded on the same day to minimize substantial day-to-day variation in the experimental results. To

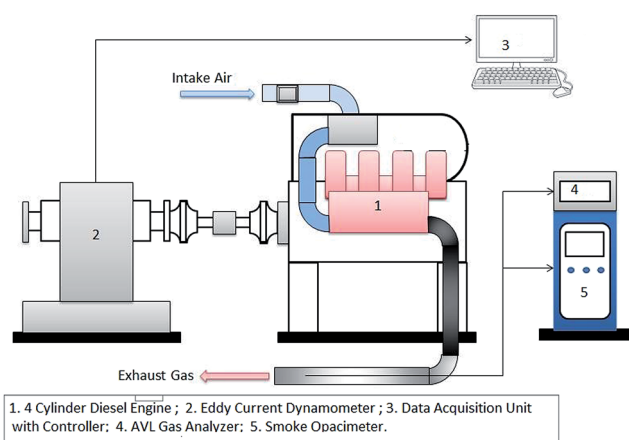


Fig. 1 Experimental set-up.

Table 5 Engine specification

Engine type	4 Stroke diesel engine
Number of cylinders	4 in-line, longitudinal
Cylinder bore × stroke	91.1 × 95 mm
Displacement	2477 cm <sup>3</sup>
Compression ratio	21 : 1
Combustion chamber	Swirl type
Rated power	65 kW at 4200 rpm
Torque	185 Nm, at 2000 rpm
Valve mechanism	Single overhead camshaft (SOHC)
Injection pressure (kg cm <sup>-2</sup> )	157 bar
Aspiration	Turbo charged
Fuel system	Distributor type injection pump
Cooling system	Radiator cooling
Lubrication system	Pressure feed, full flow filtration
Test conditions	Specifications
10% load-1000 rpm	TC1
15% load-1000 rpm	TC2
10% load-1500 rpm	TC3
15% load-1500 rpm	TC4

measure the fuel flow rate, a positive-displacement type flow meter (KOBOLD ZOD) was installed. For recording the engine test data a REO-dCA data acquisition system was incorporated. For exhaust emission analysis, an AVL DICOM 4000 gas analyzer was used to measure the concentration of CO, HC and NO<sub>x</sub>. Smoke opacity measurements were recorded with an AVL Di-Smoke 4000. The measurement range and resolution for both of the instruments are given in Table 6.

## 2.6. Accuracies and uncertainty analysis

Table 7 provides the accuracy values of the measured quantities that were used during the experiment. Uncertainties in any experimental procedure occur depending on the experimental conditions, instrument calibrations, observation, data input, test assembly, *etc.* Therefore, uncertainty analysis is a significant technique to validate the accuracy of the experimental results. In this experiment, percentage uncertainty of all measured quantities were computed by considering the percentage uncertainties of the equipment. Besides, the relative uncertainty of BSFC was determined by means of the linearized

Table 6 Specification of exhaust gas analyzer

Method	Measured component	Range	Resolution
<b>AVL exhaust gas analyser</b>			
Non-dispersive infrared	CO	0.10% vol	0.01 vol%
Non-dispersive infrared	Unburned HC	0–20 000 ppm vol	1 ppm
Electrochemical	NO <sub>x</sub>	0–5000 ppm vol	1 ppm
<b>Smoke opacimeter</b>			
Photodiode detector	Opacity%	0–100%	0.10%

approximation method of uncertainty.<sup>34</sup> Uncertainty percentages are also shown in Table 7.

## 3. Results and discussion

### 3.1. Fuel property analysis

Fuel property analysis had been conducted as part of the investigation to have a prediction about the quality of sample fuel blends prior to the engine test. Table 8 features fuel properties of the fuel blends. All of the blends used in this experiment also meet the ASTM D7467 specification. Excessive density of any fuel results in higher viscosity, which has significant influence in spray atomization efficiency, resulting in poor combustion with formation of engine deposits and higher exhaust emissions.<sup>9</sup> Among the sample fuels, all biodiesel blends showed higher density and viscosity, whereas, GTL blends showed lower values of these two parameters, than those of diesel. J10, J20, AL10 and AL20 demonstrated about 4.56%, 9.12%, 8.94% and 12.19% increased kinetic viscosity than diesel, whereas, G10 and G20 showed about 1.15% and 1.64% lower values than diesel. Lower kinematic viscosity of fuel ensures less resistance while flowing through the fuel system and it also leads to better fuel atomization.<sup>35</sup>

The flash point maintains an inverse relation to fuel volatility.<sup>36</sup> A higher flash point ensures safety of fuel for handling, storage and prevention from unexpected ignition during combustion. J10, J20, AL10, AL20, G10 and G20 demonstrated higher flash points of about 8.63%, 14.38%, 2.88%, 10.1%, 5.76% and 20.14%, respectively, than diesel. In the case of the calorific value, J10, J20, AL10 and AL20 demonstrated about 1.13%, 2.37%, 1.3% and 2.49% lower values than diesel, whereas, G10 and G20 showed higher values by about 0.82% and 1.28% compared to diesel. The higher calorific value of any fuel is desired because it favors the heat release during combustion and improves engine performance.<sup>9</sup>

CN is a measure of a fuel's auto-ignition quality characteristics. J10, J20, AL10, AL20, G10 and G20 demonstrated higher CN by about 14.3%, 18.36%, 8.16%, 14.3%, 20.4% and 32.65%, respectively, compared to diesel.

The oxidation stability values for J10, J20, AL10, AL20, G10 and G20 were 39.12 h, 36.75 h, 17.1 h, 13.55 h, 44.12 h and 48.25 h, respectively, which meet the ASTM D7467 specification.

### 3.2. Engine performance test

**3.2.1 Brake specific fuel consumption (BSFC) and brake specific energy consumption (BSEC).** Fig. 2 illustrates the variation of the BSFC values of all fuels. It was observed that the all biodiesel blends showed higher BSFC values, whereas, GTL blends showed lower values, compared to the reference fuel diesel. On average, J10, J20, AL10 and AL20 showed higher BSFC values about 5.01%, 10.71%, 6.62% and 12.18%, whereas, G10 and G20 showed lower values of BSFC approximately 8.65% and 12.26%, respectively, when compared to those of diesel.

The improvement in BSFC for GTL blends can be illustrated by the combustion phenomena and fuel characteristics. For fuel delivered on a fixed volumetric basis, the amount of fuel

Table 7 List of the accuracy of measuring component and the uncertainty

Measured components	Measurement techniques	Measuring range	Accuracy	Uncertainty
Load	Strain gauge type load cell	0–600 N m	±0.1 N m	
Speed	Magnetic pick up type	0–6000 rpm	±1 rpm	
Time	—	—	±0.1 s	
Fuel flow measurement	Positive displacement gear wheel flow meter	0.5–36 L h <sup>-1</sup>	±0.04 L h <sup>-1</sup>	
CO	Non-dispersive infrared	0–10% by vol	0.01 vol%	±0.01 vol%
HC	Non-dispersive infrared	0–20 000 ppm	±1 ppm vol	±1 ppm
NO <sub>x</sub>	Electrochemical	0–5000 ppm	±1 ppm vol	±5 ppm
Smoke opacity	Photodiode detector	0–100%	0.1%	±0.5%

Table 8 Physicochemical properties of the sample fuels

Properties	Diesel	J10	J20	AL10	AL20	G10	G20
Density kg m <sup>-3</sup>	829.6	832.6	835.1	835.3	840.1	821.83	815.8
Kinematic viscosity at 40 °C (mm <sup>2</sup> s <sup>-1</sup> )	3.075	3.21	3.35	3.45	3.85	3.045	3.025
Calorific value	44.46	43.96	43.406	43.88	43.354	44.816	45.026
Cetane number	49	56	58	53	56	59	65
Flash point (°C)	69.5	75.5	79.5	71.5	76.5	73.5	83.5
Oxidation stability at 110 °C (h)	59.1	39.12	36.75	17.1	13.55	44.12	48.25

injected in a single stroke was same for all fuels. Since the GTL blends contain a higher calorific value, it required comparatively a small quantity of fuel per stroke to produce the same power compared to biodiesel blends.<sup>37,38</sup> Besides, GTL blends could have demonstrated lower in-cylinder pressure and lower pressure rise rate, which assisted in compensating mechanical losses, resulting better combustion.<sup>39</sup> The higher BSFC values of the four biodiesel blends can be ascribed to the combined effect of lower calorific values and higher kinematic viscosity, which resulted in higher fuel consumption to produce the same output power in the constant fuel injection system, when compared to GTL blends and reference fuel diesel. Several studies<sup>16,40</sup> also confirmed that the fuel consumption of blends of diesel is increased with the decrease of the calorific value.

The brake specific energy consumption (BSEC) is introduced to compare the performance of the fuels with different calorific values. It can be defined as the product of the BSFC and calorific value of the fuel. It indicates the amount of energy consumed to produce a unit output power in one hour. In this investigation, the sample fuels have different calorific values, so BSEC is a

significant parameter to study the engine performance characteristics. Fig. 3 illustrates the variation of the BSEC values of all fuel samples. It was observed that in all test conditions biodiesel blends showed higher BSEC values, while the GTL blends showed lower values, compared to diesel. On average, J10, J20, AL10 and AL20 showed higher BSEC values by about 3.41%, 7.66%, 4.77% and 9.67%, whereas, G10 and G20 showed lower values by approximately 8.27% and 11.51%, respectively, when compared to those of diesel.

It was observed in all test conditions that both BSFC and BSEC values increase with the increase of quantity of biodiesel in blends, whereas, and GTL blends showed improvement in both BSFC and BSEC values with addition of GTL in blends. It was also observed that at higher speed test conditions (TC3 and TC4), the rate of increase of the BSFC and BSEC values for the biodiesel blends was lower than the lower speed test conditions (TC1 and TC2). This can be attributed to the higher oxygen content of biodiesel which facilitates better combustion at high temperature at high speed condition. The improvement of BSEC of J10–J20 blends compared to AL10–AL20 blends can be ascribed to the higher calorific values of JBD blends than that of ALBD blends. As described earlier, the G10–G20 blends were the best in terms of the improvement of BSFC and BSEC.

**3.2.2 Brake thermal efficiency.** Engine brake thermal efficiency is regarded as a significant performance parameter, which can be measured by the product of mechanical efficiency and net indicated thermal efficiency. Due to the effect of various loss mechanisms, such as combustion inefficiency, heat transfer and mechanical friction, the BTE of a real operating diesel cycle is usually under 50% and often far below it.<sup>41</sup> In this study, the BTE was calculated using eqn (1) where  $\eta_{bt}$  is the BTE (%),  $fc$  is the BSFC (g kW<sup>-1</sup> h<sup>-1</sup>) and CV is the calorific value of the fuel (MJ kg<sup>-1</sup>).

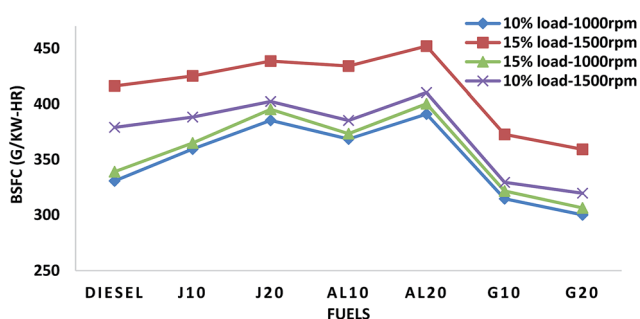


Fig. 2 Variation of BSFC of all test fuels at high idling conditions.

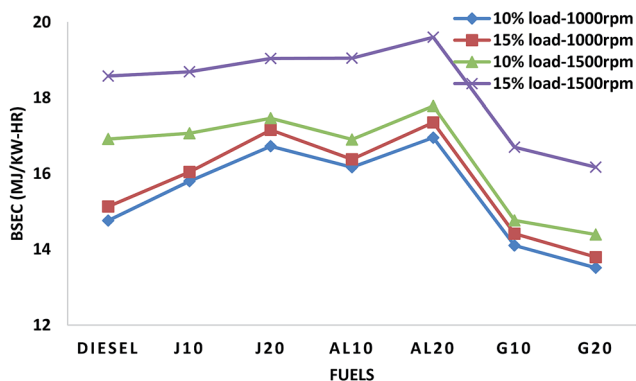


Fig. 3 Variation of BSEC of all fuels at high idling conditions.

$$\eta_{bt} = \left[ \frac{3.6 \times 10^3}{f_c \times CV} \right] \times 100\% \quad (4)$$

Fig. 4 illustrates the variation of the BTE values of all fuels. It was observed in all test modes that the biodiesel blends showed lower BTE values, while, GTL blends showed higher BTE values than diesel. It was also observed that in TC1 and TC2 the rate of decreasing BTE of the biodiesel blends with addition of biodiesel in blends is much higher than TC3 and TC4. This can be explained by the decrease of calorific values of fuel blends with addition of biodiesel quantity in blends. As described in Section 3.2.1, a higher fuel consumption is required to achieve the same output power and overcome the engine-oriented mechanical losses for fuel blends with lower calorific values. Thus, the BTE decreased significantly from J10 to J20 and AL10 to AL20 in TC1 and TC2. At higher speed conditions (TC3, TC4), a higher level of spontaneous premixing occurs at the top dead center, which induces a faster rate of combustion and thus the effect of decreasing calorific value was not as significant as at lower speed test conditions.<sup>39</sup> On average, J10, J20, AL10 and AL20 showed lower BTE by about 3.68%, 7.68%, 4.96% and 9.93%, whereas, G10 and G20 showed higher BTE by approximately 8.56% and 12.58%, respectively, when compared to those of diesel.

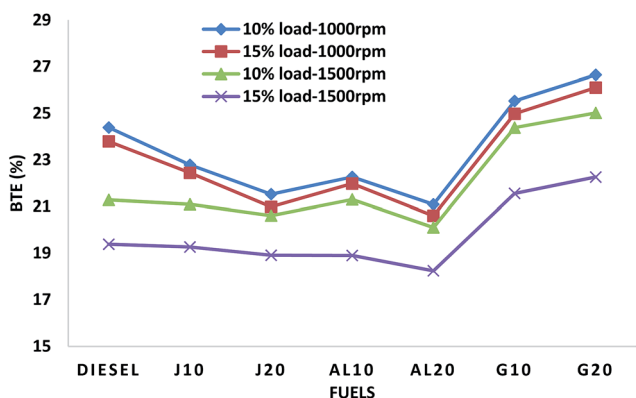


Fig. 4 Variation of BTE of all fuels at high idling conditions.

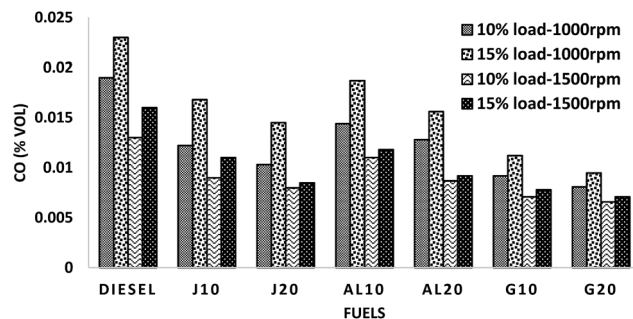


Fig. 5 Variation of CO emission of all fuels at high idling conditions.

### 3.3. Exhaust emission test

**3.3.1 CO emission.** Fig. 5 illustrates the variation of the CO emission values of all fuel samples. It was observed in all test modes that all of the blends showed lower CO emission than diesel, but G10 and G20 showed greater emission reduction compared to all of those. On average, J10, J20, AL10, AL20, G10 and G20 showed lower CO emissions by about 29.12%, 39.81%, 25.36%, 33.71%, 48.25% and 51.38%, respectively, when compared to those of diesel.

The mysteries of CO emission reduction of GTL blends can be explained by looking at the fuel properties and combustion phenomena. Significant fuel characteristics of GTL, like higher hydrogen-carbon ratio, higher CN and very low aromatic content assist in improved combustion and thus cause reduction of CO emission.<sup>9</sup> The higher CN of G10–G20 could have induced shortening of ignition delay that resulted less number of over-lean zones. Besides, the lower distillation temperature of GTL fuel induces rapid vaporization, which reduces the probability of flame quenching and thus ensures lower CO emission.<sup>39,42</sup> In case of the other four blends, lower CO emissions can be explained by the combined effect of the higher oxygen content and higher CN.<sup>43</sup> Higher CN results short ignition delay, leading towards better combustion. Moreover, the short ignition delay can also be induced by a longer chain length of biodiesel and thus improves combustion process.<sup>1</sup> High oxygen content ensures proper in-cylinder temperature, which also facilitates complete combustion.<sup>44,45</sup>

**3.3.2 HC emission.** The major reasons behind the formation of HC emission in CI engines are the over-lean fuel mixture (excessive air-fuel ratio) throughout the ignition delay period,

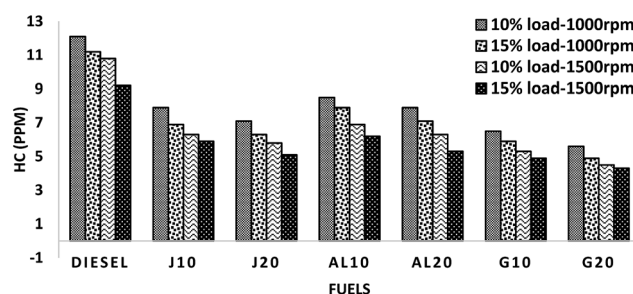


Fig. 6 Variation of HC emission of all fuels at high idling conditions.

improper mixing of fuel adjacent to the spray core at the time of combustion and especially the occurrence of wall quenching of flames due to the impingement of fuel spray on the peripheral areas of the combustion chamber.<sup>39</sup> Fig. 6 illustrates the variation of the HC emission values of all fuel blends. It had been observed in all test modes that all fuels showed lower HC emission values than diesel. On average, J10, J20, AL10, AL20, G10 and G20 showed lower HC emissions by about 33.65%, 40.27%, 29.67%, 35.46%, 44.81% and 51.43%, respectively, when compared to those of diesel.

Like for CO emission, reduction of HC emission can be explained using the same parameters. The higher CN of G10–G20 fuel blends shortens the ignition delay, which prevents the formation of the over-lean regions. Lower distillation temperature of GTL ensures a proper pace of evaporation and mixing with air to constitute a more effective combustible charge, which results in less unburned HC in the exhaust emission.<sup>42,46</sup> In case of the other four blends, the inherent higher oxygen content of biodiesel induced some advantageous conditions, such as, post-flame oxidation, higher flame speed, *etc.* throughout the air–fuel interactions, especially in the fuel-rich regions, which ensured the proper oxidation of the unburned HC and thus resulting in significant HC emission reduction.<sup>47</sup>

**3.3.3 NO<sub>x</sub> emission.** In a CI engine, the formation of NO<sub>x</sub> can be illustrated by the Zeldovich mechanism.<sup>48</sup> During the combustion process, higher temperature disengages molecular bonds of nitrogen, which initiates a series of reactions with oxygen and thus account for the occurrence of thermal NO<sub>x</sub>. Formation of NO<sub>x</sub> in the flame front and in the post-flame gases depends on the oxygen content, in-cylinder temperature and residence time.

Fig. 7 illustrates the variation of the emission values of all fuels. It was observed in all test modes that J10–J20 and AL10–AL20 blends demonstrate higher NO<sub>x</sub> emission, whereas G10–G20 showed lower NO<sub>x</sub> emission values, when compared to diesel. On average, J10, J20, AL10 and AL20 showed higher NO<sub>x</sub> emission by about 2.83%, 7.44%, 5.65% and 9.81%, whereas, G10 and G20 showed lower NO<sub>x</sub> emission by approximately 3.89% and 6.85%, respectively, when compared to those of diesel.

The diminution of NO<sub>x</sub> emission of G10–G20 can be illustrated by the influence of fuel properties in combustion

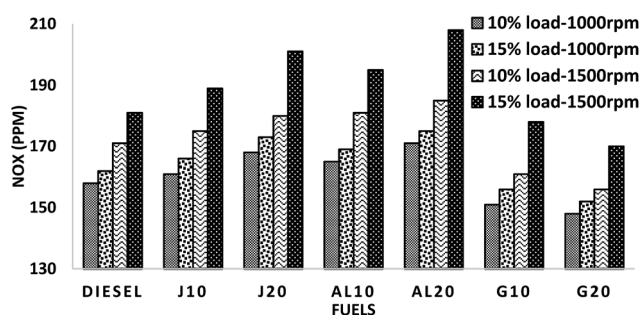


Fig. 7 Variation of NO<sub>x</sub> emission of all test fuels at high idling conditions.

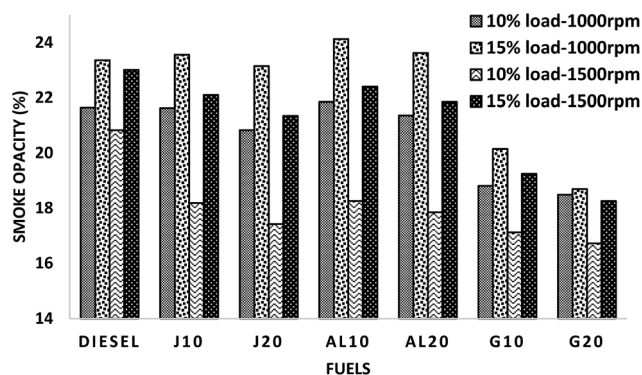


Fig. 8 Variation of smoke opacity of all fuels at high idling conditions.

phenomena and exhaust emission. The higher CN of G10–G20 induced shorter ignition delay, followed by a lesser premixed charge, which resulted in a lower combustion temperature and pressure.<sup>39,42</sup> It led towards less thermal NO<sub>x</sub> formation. Significant lower aromatic contents of GTL fuel also influenced G10–G20 blends, which prompted to maintain a lower local adiabatic flame temperature and thus assists in NO<sub>x</sub> reduction.<sup>37,49</sup> Several research studies had revealed an increase of NO<sub>x</sub> emission in biodiesel or diesel–biodiesel blends with the increase in unsaturation percentage and on the diminution of the chain length.<sup>50,51</sup> In the case of the other four blends, higher NO<sub>x</sub> was observed in all test modes because of their high oxygen content and a higher “premixed part” during combustion, where NO<sub>x</sub> is primarily formed.<sup>52</sup>

**3.3.4 Smoke emission.** Smoke is definitely an undesirable by-product, which is constituted primarily because of the incomplete combustion of hydrocarbon fuel in a C.I. engine. “Smoke opacity” is one of the most common terms to forecast the tendency of soot formation during combustion of any test fuel.<sup>53</sup> Fig. 8 illustrates the variation of smoke emission values of all fuel blends with the reference diesel fuel. It was observed in all four test modes that all of the sample fuels showed lower smoke emission than diesel. Overall, GTL blends showed higher emission reduction compared to biodiesel blends. On average, J10, J20, AL10, AL20, G10 and G20 showed lower smoke emissions by about 3.79%, 6.87%, 2.49%, 4.69%, 15.21% and 18.78%, respectively, when compared to those of diesel.

This reduction in smoke emissions in GTL blends can be explained by the combined effect of the absence of aromatics (regarded as soot predecessors), low sulfur content and higher hydrogen to carbon ratio of GTL fuel.<sup>2,39</sup> The diminution of the smoke for biodiesel blends can be attributed to the higher oxygen content, associated with lower sulfur content and impurities.<sup>53</sup>

## 4. Conclusion

In this study, production of ALBD and JBD was performed. Six blends of J10, J20, AL10, AL20, G10 and G20 were used in a comparative investigation in terms of the fuel properties, engine performance and exhaust emission than diesel. Four

engine test conditions were selected for the in-depth analysis of these blends.

- The produced ALBD and JBD showed improvement of fuel properties compared to those of their crude oil. The biodiesel blends showed further improvement in properties like density, kinematic viscosity, calorific value, oxidation stability, *etc.* compared to neat biodiesel. Unlike, diesel–biodiesel blends, GTL–diesel blends showed improvement of fuel properties, such as, lower density and kinematic viscosity, but higher calorific values and cetane number, with increased quantity of GTL in blends.

- It can be deduced from the engine performance–emission results of all sample fuel blends that all of them are eligible for running on unmodified C.I. engines.

- The engine performance test result with all four test conditions showed that G10–G20 showed higher BTE (*ca.* 8.56–12.58%), whereas, lower BSFC and BSEC (*ca.* 8.65–12.26% and 8.27–11.51%, respectively), compared with those of diesel. On average, J10–J20 and AL10–AL20 demonstrated higher BSFC (*ca.* 5.01–10.71% and 6.62–12.18%), higher BSEC (*ca.* 3.41–7.66% and 4.77–9.67%), whereas, lower BTE (*ca.* 3.68–7.68% and 4.96–9.93%, respectively), compared to those of diesel.

- Exhaust emission experiments with all four test conditions revealed significant reduction for GTL blends than the other fuels. On average, G10–G20 showed reduction in CO, HC, NO<sub>x</sub> and smoke emission (*ca.* 48.25–51.38%, 44.81–51.43%, 3.89–6.85% and 15.21–18.78%, respectively), compared to diesel. On average, J10–J20 and AL10–AL20 demonstrated higher NO<sub>x</sub> (*ca.* 2.83–7.44% and 5.65–9.81%), whereas lower CO (*ca.* 29.12–39.81% and 25.36–33.71%), HC (*ca.* 33.65–40.27% and 29.67–35.46%), smoke (*ca.* 3.79–6.87% and 2.49–4.69%, respectively), than those of diesel.

In-detail analysis of the outcome of this study has heightened the possibility of commercial application of all of these alternative fuel blends. These fuel blends may comply with the upcoming strict emission regulation and also contribute to better engine performance features ever cherished by the automobile manufacturers.

## Abbreviations

JBD	<i>Jatropha curcas</i> biodiesel
ALBD	Alexandrian laurel biodiesel
GTL	Gas-to-liquid fuel
BTE	Brake thermal efficiency
BSEC	Brake specific energy consumption
CO	Carbon monoxides
HC	Hydrocarbons
NO <sub>x</sub>	Nitrogen oxides
CN	Cetane number
FFA	Free fatty acid
GC	Gas chromatography
J10	10% JBD + 90% diesel
J20	20% JBD + 80% diesel
AL10	10% ALBD + 90% diesel
AL20	20% ALBD + 80% diesel

G10	10% GTL + 90% diesel
G20	20% GTL + 80% diesel
SN	Saponification number
IV	Iodine value
PPM	Parts per million
RPM	Rotation per minute
FT	Fischer–Tropsch

## Acknowledgements

The authors would like to acknowledge the University of Malaya for financial support through a High Impact Research grant titled: “Clean Diesel Technology for Military and Civilian Transport Vehicles” having grant number UM.C/HIR/MOHE/ENG/07.

## References

- 1 J. Xue, T. E. Grift and A. C. Hansen, *Renewable Sustainable Energy Rev.*, 2011, **15**, 1098–1116.
- 2 M. Lapuerta, O. Armas, J. J. Hernández and A. Tsolakis, *Fuel*, 2010, **89**, 3106–3113.
- 3 M. Mofijur, H. Masjuki, M. Kalam and A. Atabani, *Energy*, 2013, **55**, 879–887.
- 4 P. Rao, *World academy of science, engineering and technology*, 2011, vol. 75, pp. 855–868.
- 5 O. P. R. van Vliet, A. P. C. Faaij and W. C. Turkenburg, *Energy Convers. Manage.*, 2009, **50**, 855–876.
- 6 S. S. Gill, A. Tsolakis, K. D. Dearn and J. Rodríguez-Fernández, *Prog. Energy Combust. Sci.*, 2011, **37**, 503–523.
- 7 O. O. James, B. Chowdhury, M. A. Mesubi and S. Maity, *RSC Adv.*, 2012, **2**, 7347–7366.
- 8 A. J. Velaers and S. d. Goede, *SAE Int. J. Fuels Lubr.*, 2013, DOI: 10.4271/2013-01-1136.
- 9 H. Sajjad, H. H. Masjuki, M. Varman, M. A. Kalam, M. I. Arbab, S. Imtenan and S. M. A. Rahman, *Renewable Sustainable Energy Rev.*, 2014, **30**, 961–986.
- 10 S. H. Park, D. Lee and C. S. Lee, *Proc. Inst. Mech. Eng., Part D*, 2014, **228**, 85–93.
- 11 G. Moon, Y. Lee, K. Choi and D. Jeong, *Fuel*, 2010, **89**, 3840–3846.
- 12 O. Armas, K. Yehliu and A. L. Boehman, *Fuel*, 2010, **89**, 438–456.
- 13 M. Oguma, S. Goto, K. Oyama, K. Sugiyama and M. Mori, *SAE Tech. Pap. Ser.*, 2002, DOI: 10.4271/2002-01-1706.
- 14 C. Carraretto, A. Macor, A. Mirandola, A. Stoppato and S. Tonon, *Energy*, 2004, **29**, 2195–2211.
- 15 H. Aydin and H. Bayindir, *Renewable Energy*, 2010, **35**, 588–592.
- 16 E. Buyukkaya, *Fuel*, 2010, **89**, 3099–3105.
- 17 J. Song and C. Zhang, *Proc. Inst. Mech. Eng., Part D*, 2008, **222**, 2487–2496.
- 18 M. Gumus and S. Kasifoglu, *Biomass Bioenergy*, 2010, **34**, 134–139.
- 19 P. Sahoo, L. Das, M. Babu, P. Arora, V. Singh, N. Kumar and T. Varyani, *Fuel*, 2009, **88**, 1698–1707.

- 20 H. Sajjad, H. Masjuki, M. Varman, M. Kalam, M. Arbab, S. Imtenan and M. Rashed, *RSC Adv.*, 2014, **4**, 44529–44536.
- 21 A. S. Khan, N. N. Clark, M. Gautam, W. S. Wayne, G. J. Thompson and D. W. Lyons, *J. Air Waste Manage. Assoc.*, 2009, **59**, 354–359.
- 22 N. N. Clark, M. Gautam, W. S. Wayne, W. Riddle, R. D. Nine, D. W. Lyons and S. Xu, Examination of a Heavy Heavy-Duty Diesel Truck Chassis Dynamometer Schedule, *SAE Tech. Pap. Ser.*, 2004, DOI: 10.4271/2004-01-2904.
- 23 N. Pekula, B. Kuritz, J. Hearne, A. Marchese and R. Hesketh, The effect of ambient temperature, humidity, and engine speed on idling emissions from heavy-duty diesel trucks, *SAE Tech. Pap. Ser.*, 2003, DOI: 10.4271/2003-01-0290.
- 24 C.-J. Brodrick, H. A. Dwyer, M. Farshchi, D. B. Harris and F. G. King Jr, *J. Air Waste Manage. Assoc.*, 2002, **52**, 1026–1031.
- 25 S. M. A. Rahman, H. H. Masjuki, M. A. Kalam, M. J. Abedin, A. Sanjid and H. Sajjad, *Energy Convers. Manage.*, 2013, **74**, 171–182.
- 26 M. M. Roy, W. Wang and J. Bujold, *Appl. Energy*, 2013, **106**, 198–208.
- 27 S. M. A. Rahman, H. H. Masjuki, M. A. Kalam, M. J. Abedin, A. Sanjid and H. Sajjad, *Energy Convers. Manage.*, 2013, **76**, 362–367.
- 28 S. Rahman, H. Masjuki, M. Kalam, M. Abedin, A. Sanjid and M. M. Rahman, *Renewable Energy*, 2014, **68**, 644–650.
- 29 M. Canakci and J. Van Gerpen, *Trans. Am. Soc. Agric. Eng.*, 2001, **44**, 1429–1436.
- 30 M. Y. Koh and T. I. Mohd Ghazi, *Renewable Sustainable Energy Rev.*, 2011, **15**, 2240–2251.
- 31 I. Rizwanul Fattah, H. Masjuki, M. Kalam, M. Wakil, A. Ashraful and S. Shahir, *Energy Convers. Manage.*, 2014, **83**, 232–240.
- 32 K. Agee, *Fundamentals of Gas to Liquids*, London: Petroleum Economist, 2nd edn, 2005, pp. 30–31.
- 33 M. Mohibbe Azam, A. Waris and N. Nahar, *Biomass Bioenergy*, 2005, **29**, 293–302.
- 34 M. Mofijur, H. H. Masjuki, M. A. Kalam, A. E. Atabani, I. M. R. Fattah and H. M. Mobarak, *Ind. Crops Prod.*, 2014, **53**, 78–84.
- 35 M. I. Arbab, H. H. Masjuki, M. Varman, M. A. Kalam, S. Imtenan and H. Sajjad, *Renewable Sustainable Energy Rev.*, 2013, **22**, 133–147.
- 36 M. Arbab, H. Masjuki, M. Varman, M. A. Kalam, H. Sajjad and S. Imtenan, *RSC Adv.*, 2014, **4**, 37122–37129.
- 37 A. Abu-Jrai, A. Tsolakis, K. Theinnoi, R. Cracknell, A. Megaritis, M. L. Wyszynski and S. E. Golunski, *Energy Fuels*, 2006, **20**, 2377–2384.
- 38 K. Yehliu, A. L. Boehman and O. Armas, *Fuel*, 2010, **89**, 423–437.
- 39 H. Yongcheng, Z. Longbao, W. Shangxue and L. Shenghua, *Proc. Inst. Mech. Eng., Part D*, 2006, **220**, 827–835.
- 40 M. Lapuerta, O. Armas and J. Rodriguez-Fernandez, *Prog. Energy Combust. Sci.*, 2008, **34**, 198–223.
- 41 J. B. Heywood, *Internal Combustion Engine Fundamentals*, McGraw-Hill, New York, 2002.
- 42 T. Wu, Z. Huang, W.-g. Zhang, J.-h. Fang and Q. Yin, *Energy Fuels*, 2007, **21**, 1908–1914.
- 43 J. B. Hirkude and A. S. Padalkar, *Appl. Energy*, 2012, **90**, 68–72.
- 44 E. Cecerle, C. Depcik, A. Duncan, J. Guo, M. Mangus, E. Peltier, S. Stagg-Williams and Y. Zhong, *Energy Fuels*, 2012, **26**, 2331–2341.
- 45 Y. Di, C. Cheung and Z. Huang, *Sci. Total Environ.*, 2009, **407**, 835–846.
- 46 H. Wang, H. Hao, X. Li, K. Zhang and M. Ouyang, *Appl. Energy*, 2009, **86**, 2257–2261.
- 47 A. N. Ozsezen, M. Canakci, A. Turkcan and C. Sayin, *Fuel*, 2009, **88**, 629–636.
- 48 I. M. Rizwanul Fattah, M. A. Kalam, H. H. Masjuki and M. A. Wakil, *RSC Adv.*, 2014, **4**, 17787–17796.
- 49 L. Xinling and H. Zhen, *Sci. Total Environ.*, 2009, **407**, 2234–2244.
- 50 S. K. Hoekman and C. Robbins, *Fuel Process. Technol.*, 2012, **96**, 237–249.
- 51 G. Knothe, *Fuel Process. Technol.*, 2005, **86**, 1059–1070.
- 52 D. Rakopoulos, *Fuel*, 2013, **105**, 603–613.
- 53 S. Imtenan, M. Varman, H. H. Masjuki, M. A. Kalam, H. Sajjad, M. I. Arbab and I. M. Rizwanul Fattah, *Energy Convers. Manage.*, 2014, **80**, 329–356.